Inorg. Chem. 1993, *32*, 3265–3269 3265

A Study of High-Valent Manganese in Aqueous H_3PO_4: Disproportionation of $[Mn^{III}Mn^{IV}(\mu\text{-}O)_2(bpy)_4]^{3+}$

Joseph E. Sarneski,[*,†] Linda J. Brzezinski,[†] Brandon Anderson,[†] Mary Didiuk,[†] Rajesh Manchanda,[‡] Robert H. Crabtree,[‡] Gary W. Brudvig,[‡] and Gayle K. Schulte[‡]

Departments of Chemistry, Fairfield University, Fairfield, Connecticut 06430, and Yale University, New Haven, Connecticut 06511

Received July 31, 1992

The mixed-valence dimer $[Mn^{III}Mn^{IV}(\mu\text{-}O)_2(bpy))_4]^{3+}$ (**1**; bpy = 2,2′-dipyridyl) has been shown to disproportionate in aqueous H_3PO_4. One product, $[Mn^{IV}_2(\mu\text{-}O)_2(\mu_2\text{-}HPO_4)(bpy)_2(H_2PO_4)_2]$ (**2**), was isolated and characterized earlier (*Inorg. Chem.* **1991**, *30*, 2833). Here a manganese(III) product has been characterized crystallographically as $[Mn^{III}(bpy)(HPO_4)(H_2PO_4)]_x$ (**3**). **3** is a polymeric material which crystallizes in the space group $P\bar{1}$ (No. 2) with a = 8.069(1) Å, b = 8.672(2) Å, c = 10.751(1) Å, α = 109.91(2)°, β = 102.04(1)°, and γ = 90.20(9)°. A total of 1569 unique data with $I \geq 3(\sigma)I$ were refined to values of R and R_w of 3.9 and 4.3%, respectively. The Mn(III) ions, bridged by two μ_2-phosphate ligands, are 4.93 Å apart; each Mn(III) atom is bridged in this manner to two other $[Mn^{III}(bpy)(HPO_4)(H_2PO_4)]$ formula units leading to a polymeric array. The aqueous chemistry of **2** and **3** has been characterized by UV–vis and EPR spectroscopy. The electrochemistry of the (IV,IV) dimer **2** in phosphate buffer shows that the complex decomposes on reduction to give the mixed-valence bis(μ-oxo) manganese dimer **1**. Support for the electrochemical formation of **1** from **2** in phosphate buffer was obtained from the zero current potential curve. The Mn(III)–bpy phosphate (**3**) is found to disproportionate spontaneously to **1** and Mn(II) upon dissolution in phosphate buffer; for solutions of **2** or **3** in 0.1 M H_3PO_4 electrochemistry typical of **1** is observed. The temperature-dependent magnetic susceptibility shows strong antiferromagnetic coupling for the (IV,IV) dimer **2** with J = 79 cm^{-1} ($\mathcal{H} = JS_1 \cdot S_2$). The Mn(III) complex **3** shows weak antiferromagnetic coupling, consistent with the long Mn–Mn distance of 4.93 Å.

The chemistry of high-valent manganese has been an area of intense research interest in recent years due to the involvement of this element in a number of important biological processes which utilize redox-active manganese centers. We are interested in the role that Mn plays in the accumulation of oxidizing equivalents in the water-oxidation catalyst in photosystem II (PS II); other redox bioinorganic chemistry of manganese has been summarized in recent reviews.[1–4]

Because the manganese cluster in the oxygen evolution center uses water as its substrate, it is important to understand the factors which can lead to stabilization of high manganese oxidation states in aqueous media. Collins *et al.* have recently reported the design of macrocyclic tetraamide ligands which have yielded a Mn(V)–oxo complex; their efforts have also provided considerable insight into the design of oxidation resistant ligand systems.[5]

We have been investigating the stabilization of high-valence manganese in aqueous media through binding of the oxidation-resistant ligand PO_4^{3-} and earlier reported[6] the isolation of the bis(μ-oxo)(μ-phosphate)dimanganese(IV,IV) dimer **2** from a solution of the mixed-valence (III,IV) dimer $[(bpy)_2Mn(\mu\text{-}O)_2\text{-}Mn(bpy)_2]^{3+}$ (**1**) in 0.1 M H_3PO_4. Our attention was focused on this disproportionation reaction because the classic 16-line EPR signal of **1** is absent in 0.1 M H_3PO_4 solution; the solution is EPR silent with no trace of the six-line Mn(II) EPR spectrum. Also intriguing was the quantitative reversibility of this reaction to regenerate the 16-line EPR spectrum (and visible spectrum) of **1** upon addition of pH 4.5 bpy buffer to the 0.1 M H_3PO_4 solution. This report provides a detailed study of the chemistry of this system and the isolation and characterization of a Mn(III) product obtained from this solution.

Experimental Methods

$[Mn^{III}(bpy)(H_2PO_4)(HPO_4)]_x$ (3). From the previously reported procedure (this preparation represents a continuation of the same experiment described in ref 6, footnote 14) for the isolation of **2** from **1**, a second, pure red material could be isolated by careful collection of fractions from the continuing precipitation, which proceeds slowly with the evaporation of the solvent. Middle fractions contain a mixture of **2** and **3**. Later fractions contain pure **3**; when the solution volume had reached ~75 mL, 0.43 g (1.06 mmol) of pure **3** was isolated (45% yield based on preparative data given in ref 6; also it should be noted that the correct yield of **2** is 25% and not 12% as stated in ref 6). Anal. Calc for $C_{10}H_{11}N_2O_8P_2Mn$: C, 29.72; H, 2.74; N, 6.93; P, 15.33; Mn, 13.60. Found: C, 29.33; H, 2.85; N, 6.86; P, 14.99; Mn, 13.53. A gram equivalent weight of 365 was determined by iodometric titration (theoretical value = 404).

A second, more direct synthesis of **3** was developed. To a solution of 0.736 g (3.00 mmol) of $Mn(CH_3CO_2)_2\cdot 4H_2O$ and 0.588 g (3.76 mmol) of 2,2′-bipyridine (bpy) in 300 mL of 0.1 M H_3PO_4 was added 0.132 g (0.83 mmol) of $KMnO_4$ dissolved in 60 mL of water. Slow evaporation of this solution to ≈75 mL yielded 0.509 g of crystalline pink solid which is the monohydrate of **3** (30% yield). Anal. Calc for $C_{10}H_{13}N_2O_9P_2Mn$: C, 28.45; H, 3.10; N, 6.64; P, 14.68. Found: C, 28.10; H, 3.26; N, 6.48; P, 14.70. The gram equivalent weight was found by iodometric titration to be 400, in good agreement with the theoretical value of 422 for a monohydrate, **3**·H_2O.

Measurements. Cyclic voltammograms were recorded in solutions made with doubly deionized water using a PAR 273 potentiostat. Glassy-carbon working electrodes were activated in 0.1 M H_2SO_4 by cycling between potentials of +1.8 V (30 s) and −0.2 V (15 s) after polishing with alumina.[7] The auxiliary electrode was a Pt wire with a saturated calomel electrode (SSCE) reference electrode. The concentration of the complex was 1–2 mM. The solutions were buffered with 0.1 M phosphate or bpy. The pH was adjusted after addition of the metal complex using 0.1 M NaOH or 0.1 M HNO_3. EPR measurements were performed as previously described.[7] Variable-temperature magnetic susceptibility data were measured on finely powdered samples at the Francis Bitter National

---

[†] Fairfield University.

[‡] Yale University.

(1) Brudvig, G. W.; Crabtree, R. H. *Prog. Inorg. Chem.* **1989**, *37*, 99.

(2) Christou, G. *Acc. Chem. Res.* **1989**, *22*, 328.

(3) Pecoraro, V. L. *Photochem. Photobiol.* **1988**, *48*, 249.

(4) Wieghardt, K. *Angew. Chem., Int. Ed. Engl.* **1989**, *28*, 1153.

(5) Collins, T. J.; Gordon-Wylie, S. W. *J. Am. Chem. Soc.* **1989**, *111*, 4511. Collins, T. J.; Kostka, K. L.; Uffelman, E. S.; Weinberger, T. L. *Inorg. Chem.* **1991**, *30*, 4204.

(6) Sarneski, J. E.; Didiuk, M.; Thorp, H. H.; Brudvig, G. W.; Crabtree, R. H.; Schulte, G. K. *Inorg. Chem.* **1991**, *30*, 2833.

(7) Thorp, H. H.; Sarneski, J. E.; Brudvig, G. W.; Crabtree, R. H. *J. Am. Chem. Soc.* **1989**, *111*, 9249.

0020-1669/93/1332-3265$04.00/0

Table I. Crystallographic Data for **3**

emp form	$C_{10}H_{11}MnO_8N_2P_2$
M_r	404.09
cryst syst	triclinic
space gp	$P\bar{1}$ (No. 2)
temp, °C	23
a, Å	8.069(1)
b, Å	8.672(2)
c, Å	10.751(1)
α, deg	109.91(2)
β, deg	102.04(1)
γ, deg	90.20(9)
V, Å^3	689.4(4)
Z	2
cryst dimens, mm	0.10 × 0.05 × 0.05
cryst dens, calcd, g/cm^3	1.946
radiation, Mo Kα, Å	0.710 69
abs coeff, cm^{-1}	11.92
$2\theta_{max}$, deg	49.9
tot. no. of data	2419
no. of obsd data [$I \geq 3\sigma(I)$]	1569
no. of refinement params	208
$R = \sum\|\|F_o\| - \|F_c\|\|/\|F_o\|$	0.039
$R_w = [\sum_w(\|F_o\| - \|F_c\|)^2/\sum wF_o^2]^{1/2}$	0.043
goodness of fit	1.41

Magnet Laboratory at MIT with an SHE SQUID magnetometer. These data were corrected for sample diamagnetism. The μ_{eff} *vs* T data were fit using the program KaleidaGraph (Synergy Software, Reading, PA). Elemental analyses were performed by Galbraith Laboratories, Knoxville, TN. Visible spectra were obtained on a Perkin-Elmer Model 283 spectrophotometer. Solid-state reflectance spectra were measured on a P-E lambda-4c spectrometer using a $BaSO_4$ lined diffuse reflectance integrating sphere accessory; spectra were measured as relative reflectance of a 10% powdered mixture of manganese complex in silica gel *vs* pure silica gel.

Results and Discussion

Synthesis of 3. In an earlier communication[6] we described the disproportionation reaction of **1** in aqueous H_3PO_4 and characterized the di-μ-oxo phosphate-bridged Mn(IV) dimer, **2**, that we isolated. Because no EPR signals were observed from a solution of **1** in aqueous H_3PO_4, we postulated that a manganese(III) complex was present in solution. A Mn(III) species has now been isolated from this solution. The Mn(IV) dimer (**2**) precipitates first and continues coming out slowly as the solution volume is decreased; a number of fractions containing a mixture of **2** and **3** were collected before the pure solid **3** was isolated. **3** has the empirical formula $Mn(bpy)(H_2PO_4)(HPO_4)$.

Because this method is tedious and many fractions containing a mixture of **2** and **3** must be collected, a direct stoichiometric synthesis from Mn^{2+}, MnO_4^-, and bpy in aqueous H_3PO_4 was developed. This procedure yields pure **3**, in good yield, as a monohydrate with no evidence of contamination by the Mn(IV) dimer. The infrared spectra of **3** made by these two different methods, *i.e.* hydrated and nonhydrated forms, are essentially identical in the region 500–1400 cm^{-1}. Gram equivalent weights determined by iodometric titration for these two independent preparations of **3** support their formulation as Mn(III).

It is noteworthy that our attempts to produce the analogous Mn(IV) dimer (**2**) by similar stoichiometric synthesis have produced only **3** in good yield; this result is especially surprising since the visible spectrum of the reaction solution exhibits the 610 nm absorbance due to **2**. Interestingly, the visible spectrum of the solution containing the stoichiometric preparation of **3** also shows a weak 610 nm band, however, no detectable **2** precipitates. These observations will be discussed in greater detail in a later section on electronic spectra.

Solid-State Characterization. Structure of 3. Continued slow evaporation of a solution of **1** in 0.1 M H_3PO_4, after the (IV,IV) dimer (**2**) is allowed to precipitate and is removed, yields red crystals suitable for X-ray analysis. Crystallographic data for the structure of **3** are given in Table I. An ORTEP diagram for the manganese repeat unit, with selected bond lengths, is presented in Figure 1. The coordination geometry of the Mn atom is essentially octahedral, with the expected Jahn–Teller distortion for Mn(III) along the O3–Mn–O6 axis. The bond distances between atoms in the coordination sphere of the Mn in **3** are typical for Mn(III).

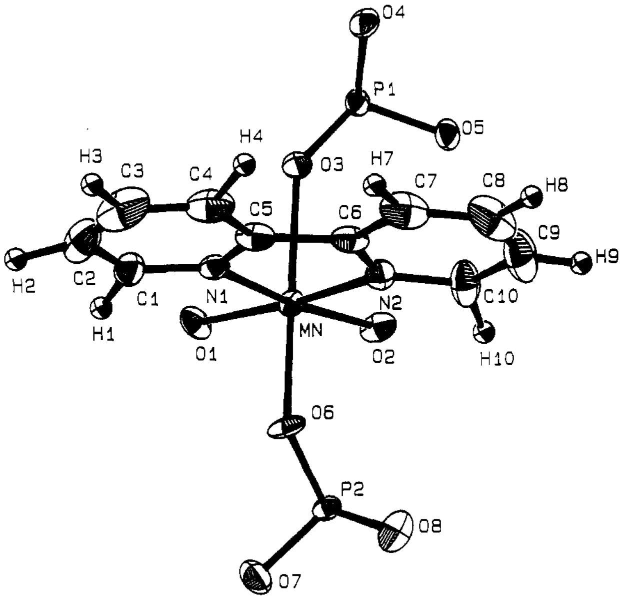

Figure 1. ORTEP of the formula unit in **3**, $[Mn^{III}(bpy)(HPO_4)(H_2PO_4)]$. Selected bond distances, in Å: Mn–O1 = 1.869(3); Mn–O2 = 1.882(4); Mn–O3 = 2.226(4); Mn–O6 = 2.135(4); Mn–N1 = 2.040(4); Mn–N2 = 2.048(4). The missing oxygen atom on each coordinated phosphate (equivalent to O1 and O2) is found in the manganese coordination sphere of an adjacent asymmetric unit to which the phosphate is bridged.

The asymmetric Mn unit presented in Figure 1 is part of a polymeric structure which makes the full formulation of the solid **3**, $[Mn(bpy)(H_2PO_4)(HPO_4)]_x$. One of the oxygen atoms on P2 in Figure 1 (not shown for sake of clarity) is the equivalent of O2 in the coordination sphere of the next Mn′ unit in the polymer, with a symmetry related phosphate on Mn′ reciprocating to contribute O2 to the coordination sphere of the first Mn; the manganese atom depicted in Figure 1 uses an oxygen atom on P1 (not shown) and O1 (from a phosphate on a second adjacent Mn) to produce a similar arrangement of two bridging phosphates linking it to a second Mn(III). This participation of each Mn atom in two separate, doubly-bridged μ_2-phosphate interactions with different Mn atoms produces the linear polymeric array shown in Figure 2 with stacking of the bpy rings visible in this chain. It is not possible to assign the positions of the three phosphate hydrogens per formula unit with any certainty on the basis of an inspection of the P–O bond distances; however, short intermolecular O···O contacts (2.54 and 2.59 Å) between phosphate oxygens on one chain with those on an adjacent chain indicate hydrogen bonding between chains. The doubly-bridged Mn–Mn distance is 4.93 Å.

Infrared Spectra. The Mn(IV) dimer, **2**, and the Mn(III) polymer, **3**, exhibit infrared absorptions at similar frequencies; however, significant differences can be seen. **2** exhibits a much broader distribution of strong peaks than **3** around 1250–850 cm^{-1} where ν(PO) bands are found; especially prominent are strong broad bands at 1200 and 950 cm^{-1} which are not present in the spectrum of **3**. Since **2** has one bridging μ_2-phosphate and two terminal monodentate phosphates, the greater complexity in its ν(PO) region would be expected relative to **3** where all phosphates are bridging. **2** also has unique broad bands of medium intensity at 652, 628, and 601 cm^{-1}. By analogy with other assignments in the literature, the band at 652 cm^{-1} could be attributed to the Mn_2O_2 stretching mode.[8] Since **3** has no μ-oxo functionalities, the absence of such bands in this region is reasonable.

---

(8) Cooper, S. R.; Calvin, M. *J. Am. Chem. Soc.* **1977**, *99*, 6623.

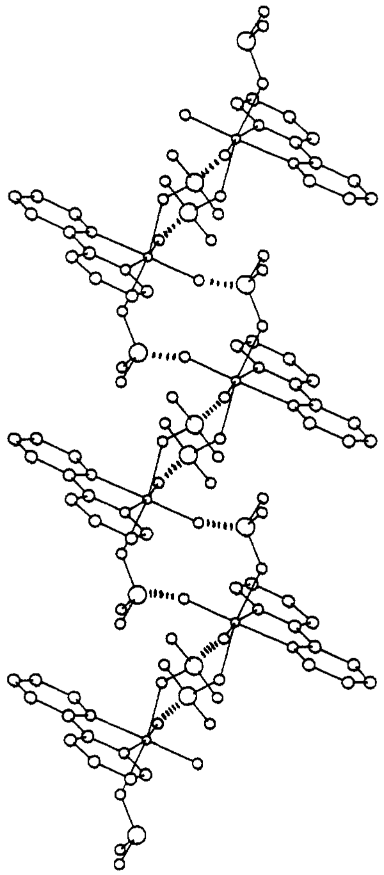

Figure 2. Packing diagram showing the polymeric nature of 3. The $[Mn^{III}(bpy)(HPO_4)(H_2PO_4)]$ formula units joined together are depicted by ···, which represent P–O phosphate covalent bonds.

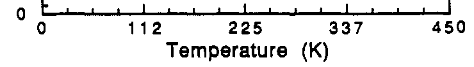

Figure 3. Temperature dependence of the magnetic moments (μ_{eff}) per dimer of Mn of 2 and 3. The data for 2 were analyzed by using the exchange Hamiltonian: $\mathcal{H} = JS_1 \cdot S_2$, where S_1 and S_2 are the spins of the Mn(III) and Mn(IV) ions, respectively. The solid line is a least-squares fit to the data using the following parameters: $J = 79$ cm^{-1} and $g = 1.81$ (a 3.3% contamination of 2 by 3 was assumed in order to reproduce the low-temperature data of 2).

Magnetism. Figure 3 shows the temperature dependence from 4.5 to 400 K of the magnetic moments (μ_{eff}, units of μ_B) for complexes 2 and 3. Complex 3 shows weak antiferromagnetic coupling of the Mn(III) ions, consistent with the long Mn···Mn separation. The high-temperature magnetic moment of 3 (6.68 μ_B) is a further demonstration that the manganese ions are in the Mn(III) oxidation state. Due to the polymeric structure of 3, we have not used an exchange Hamiltonian to evaluate the exchange coupling.

Complex 2 also shows antiferromagnetic coupling of the Mn(IV) ions. An expression for μ_{eff} was derived from the Van Vleck equation[9] and from the spin-only definition of the magnetic moment. The solid line in Figure 3 shows the best fit using a nonlinear least-squares fitting procedure. The exchange coupling constant (79 cm^{-1}) is unusually small for a di-μ-oxo-bridged Mn^{IV} dimer. A previous study of the $Mn^{IV}_2O_2$(picolinate)$_4$ complex[10] found an exchange coupling of 174 cm^{-1}, which was noted to be unusually weak for a di-μ-oxo-bridged Mn^{IV} dimer;[11] this small J coupling was attributed to the predominance of O-donor ligands in the Mn coordination sphere in contrast to other (IV,IV) dimers of predominantly N donor ligands where larger J-values are observed. Hendrickson and co-workers[10] have suggested that an increased number of π-bonding oxygen ligands in the picolinate complex increases the energy mismatch of the t_{2g} metal d_π orbitals and the bridging oxide p_π orbitals which mediate π-superexchange and hence decreases the antiferromagnetic exchange interaction. In 2, which has a Mn···Mn distance similar to that of the picolinate complex, the presence of both bridging and terminal phosphate ligands leads to a largely O coordination environment about each Mn ion and may be responsible for the anomalously weak antiferromagnetic coupling.

Solution Chemistry. Electronic Spectra and Solution Chemistry. Treatment of an aqueous solution of $[(bpy)_2Mn(\mu\text{-}O)_2Mn(bpy)_2]^{3+}$ (1) with H_3PO_4 (pH 2.3) generates a stable green solution, exhibiting a weak (ϵ = 160 M^{-1} cm^{-1}) absorption at 610 nm but now lacking the characteristic intervalence charge transfer bands of 1 in the 700–900-nm region; from this solution the (IV,IV) dimer (2) was isolated. Since the EPR spectrum of this solution provides key evidence for the lack of any significant Mn^{2+} in this solution, the simplest representation of this reaction involves a disproportionation (based on the dimeric cluster 1) with the net result described in eq 1, where the identity of the Mn(III) species

$$\underset{\mathbf{1}}{[(bpy)_2Mn^{III}(\mu\text{-}O)_2Mn^{IV}(bpy)_2]^{3+}} \xrightarrow{H_3PO_4} \underset{\mathbf{2}}{[Mn^{IV}_2(\mu\text{-}O)_2(\mu_2\text{-}HPO_4)(bpy)_2(H_2PO_4)_2]} + Mn^{III}\ \text{complex} + bpy \quad (1)$$

in solution is left undefined. While the solid-state structure of 3 is polymeric, we suspect that this is not the dominant Mn(III) species in the solution. Instead, a 1:1 Mn:bpy monomer stabilized by phosphate coordination or a (III,III) μ-oxo dimer, such as $[Mn^{III}_2(\mu\text{-}O)(\mu\text{-}H_2PO_4)_2(bpy)_2(H_2PO_4)_2]$ (4), analogous to the acetate compound that Christou has recently reported[12] to be stable in aqueous solution, may be present. Characterization of the soluble Mn(III) complex in eq 1 is complicated by the fact that the polymeric Mn(III) species 3 precipitates only after significant concentration of the solution has occured by evaporation; this raises the phosphate concentration, from initially 0.1 M, to 0.3–0.5 M at the time of precipitation.

Since both 2 and 3 are only sparingly soluble in aqueous H_3PO_4, reflectance spectra were obtained to determine the species responsible for the 610-nm band. The Mn(IV) dimer 2 exhibits the 610-nm band and also a weaker band at 750 nm in the solid state. The Mn(III) solid shows a weak, broad band centered around 800 nm and a stronger peak at 540 nm whose tail contributes to some absorption at 610 nm. From this evidence the 610-nm peak is assigned to the $Mn(IV)_2$ complex, 2. Indeed, as the (IV,IV) dimer precipitates from the original H_3PO_4 solution of 1 the 610-nm absorbance of the solution decreases.

From quantitative spectral data on a solution of 1 in 0.1 M H_3PO_4 the molar absorptivity (ϵ) of the peak at 610 nm is found to be 160 M^{-1} cm^{-1}, with a broader band occuring at 755 nm (ϵ = 60 M^{-1} cm^{-1}); however, this spectrum represents the combined absorbances of the Mn(IV) dimer 2 and the Mn(III) species in

---

(9) Van Vleck, J. H. *Theory of Electric and Magnetic Susceptibilities*; Oxford University Press: London, 1932.

(10) Libby, E.; Webb, R. J.; Streib, W. E.; Folting, K.; Huffman, J. C.; Hendrickson, D. N.; Christou, G. *Inorg. Chem.* **1989**, *28*, 4037.

(11) Thorp, H. H.; Brudvig, G. W. *New J. Chem.* **1991**, *15*, 479.

(12) Blackman, A. G.; Lobkovsky, E.; Huffman, J. C.; Christou, G. *Abstracts of Papers*, 201st Meeting of the American Chemical Society, Atlanta, GA; American Chemical Society: Washinton, DC, 1991; INOR-520.

the solution. Since the EPR spectrum of this solution indicates that there is no Mn(II) present in this solution, if one assumes that the Mn(III) is present as a dimer, such as **4**, there will be equal concentrations of **2** and **4** present. This simple model is consistent with the EPR evidence, i.e., that the solution of **1** in 0.1 M H_3PO_4 is EPR silent; strongly antiferromagnetically coupled $\mathrm{Mn^{III}_2}$ and $\mathrm{Mn^{IV}_2}$ dimers are expected to be EPR inactive, since the ground state will be spin-zero.[13] Studies were performed to determine the spectra of individual components **2** and **4** in order to interpret the aqueous chemistry and electrochemistry in phosphate media. With this simple approach we are able to better understand some of the apparent spectral inconsistencies in our attempted stoichiometric preparations of **2** and **3** (*vide supra*).

Using this model, the concentrations of **2** and **4** are half the original concentration of **1** in 0.1 M H_3PO_4, which was used to calculate the ϵ_{610} of 160 M^{-1} cm^{-1} for **1** in 0.1 M H_3PO_4; this means that $[\epsilon_{610}]_2 + [\epsilon_{610}]_4 = 320$ M^{-1} cm^{-1}. A solution of the pure (IV,IV) dimer **2** in 0.1 M H_3PO_4, while not very concentrated, gives an estimated value of 260 M^{-1} cm^{-1} for $[\epsilon_{610}]_2$; therefore, $[\epsilon_{610}]_4$ is ~60 M^{-1} cm^{-1}.

In a second method to determine the individual extinction coefficients for **2** and **4** at 610 nm, we titrated a solution of **1** in 0.1 M H_3PO_4 with a standard $KMnO_4$ solution. With the addition of permanganate, the absorbance of the 610-nm band increases indicating an increase in the concentration of the (IV,IV) species **2**; however, the reaction was not a straightforward stoichiometric conversion of the Mn(III) species to the Mn(IV) dimer **2**. The reaction of **2** with $KMnO_4$ was found to be complete within 1 min; the 610-nm absorbance was quickly measured and an aliquot of the solution taken for immediate, iodometric determination of the number of oxidizing equivalents present. In every instance, the total number of oxidizing equivalents measured after the addition of some $KMnO_4$ was considerably less than the total sum of the oxidizing equivalents put in solution from **1** and added $KMnO_4$. All the oxidizing equivalents remaining in the solution beyond those due to the initially added **1** were assumed to convert Mn(III) (**4**) to the Mn(IV) dimer (**2**). Generally, ~50% of the oxidizing equivalents from added $KMnO_4$ were lost. The missing oxidizing equivalents are presumably lost by oxidation of free bpy; when a $KMnO_4$ solution is added to bpy in 0.1 M H_3PO_4, the purple color is quickly discharged to a colorless solution indicative of the formation of Mn(II). Such oxidation of bpy in high-valent ruthenium complexes has been reported.[14]

From the increase in the 610-nm absorbance and the corresponding number of oxidizing equivalents present after each addition of $KMnO_4$, we were able to assess the amounts of **2** and **4** present in solution immediately after each addition. There are two different stoichiometric situations which could be applicable to this oxidation. If only "preformed" Mn(III) clusters (**4**) can be converted to **2** by the $KMnO_4$ oxidant, then the $KMnO_4$ would be reduced to Mn(II) as in eq 2. Because there is excess bpy in

$$\underset{\mathbf{4}}{5\mathrm{Mn^{III}_2}} + 2\mathrm{Mn^{VII}} \rightarrow \underset{\mathbf{2}}{5\mathrm{Mn^{IV}_2}} + 2\mathrm{Mn^{II}} \tag{2}$$

the starting solution (see eq 1), it is also possible for the oxidant's Mn to be incorporated into the (IV,IV) product by the stoichiometry in eq 3. The measured absorbances at 610 nm and the

$$\underset{\mathbf{4}}{3\mathrm{Mn^{III}_2}} + 2\mathrm{Mn^{VII}} \rightarrow \underset{\mathbf{2}}{4\mathrm{Mn^{IV}_2}} \tag{3}$$

simultaneous determination of the oxidizing equivalents by iodometric titration after each $KMnO_4$ addition permit estimates of $[\epsilon_{610}]_2$ and $[\epsilon_{610}]_4$ in agreement with those above and support eq 3 as appropriate to the reaction stoichiometry being observed.

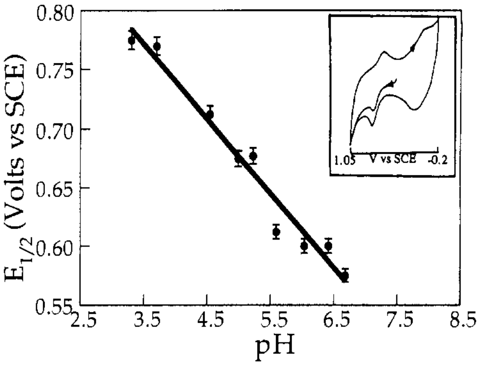

Figure 4. Pourbaix diagram of $[\mathrm{Mn^{IV}Mn^{IV}}(\mu\text{-O})_2(\mu\text{-HPO}_4)(\mathrm{bpy})_2(\mathrm{H_2PO_4})_2]$ (**2**) in 0.1 M phosphate buffer. The slope is 0.063 ± 0.01 V/pH. Inset: Cyclic voltammogram of **2** in 0.1 M phosphate buffer at pH 4.55 with scan rate 100 mV/s.

Using these ϵ_{610} data, we can better analyze the composition of our solutions in the attempted stoichiometric preparations of **2** and **3**. The attempted direct synthesis of the Mn(III) complex from Mn(II) and $KMnO_4$ shows a small absorbance at 610 nm which corresponds to ~3% of the (IV,IV) dimer in this solution. This is probably due to the accumulation of Mn(III) species with the early additions of $KMnO_4$, which are then capable of being oxidized to **4** as more $KMnO_4$ is added. Stoichiometric addition of enough $KMnO_4$ to produce the (IV,IV) dimer gives a much larger absorbance at 610 nm, but this solution is a complicated mixture of 40–50% (IV,IV) dimer and 20–40% Mn(III) with the remainder being Mn(II). Because this solution composition can vary depending on the rate of addition of $KMnO_4$, we have not pursued this effect further. It is curious that the (IV,IV) dimer (**2**) can be obtained readily from a solution of **1** in H_3PO_4, yet **2** cannot be obtained from the attempted stoichiometric (IV,IV) synthesis even though significant (IV,IV) dimer is present in solution on the basis of the intensity of the 610-nm band. We believe that this inability to isolate **2** from this procedure is attributable to the presence of significant amounts of Mn(II) in the solution from the stoichiometric synthesis. If a green solution of the (III,IV) dimer **1** in H_3PO_4, which normally precipitates the (IV,IV) dimer **2** quickly on standing, is treated with $Mn(ClO_4)_2$, the 610-nm band is immediately decreased and no (IV,IV) dimer **2** precipitates on evaporation.

Electrochemistry. The cyclic voltammogram of **2** in pH 4.55 phosphate buffer is shown in the inset of Figure 4. This complex shows two distinct redox processes, one at 0.7 V and the other at 0.0 V. The peak at 0.0 V is broad, and it is difficult to measure the peak-to-peak separation or the $E_{1/2}$ value accurately. On the other hand, the peak at 0.7 V is well-defined and sharp. The peak-to-peak separation (ΔE_p) of 110 mV indicates a quasi-reversible couple. The pH dependence of this wave is characterized in Figure 4. $E_{1/2}$ of the complex changes linearly with pH; these $E_{1/2}$ vs pH data agree well with our earlier reported characterization of the electrochemistry of **1**.[6] As pointed out in our earlier analysis,[6] the slope of 0.063 ± 0.010 V/pH unit is consistent with a coupled process involving one proton–one electron and we assigned this wave to the couple $[\mathrm{Mn^{III}Mn^{IV}}(\mu\text{-O})_2(\mathrm{bpy})_4]^{3+}/[\mathrm{Mn^{III}_2}(\mu\text{-O})(\mu\text{-OH})(\mathrm{bpy})_4]^{3+}$.[7] It is apparent from this data that the mixed-valence (III,IV) phosphate-bridged complex analogous to **2** is not a stable entity in these phosphate solutions, rather **1** is favored; the reason for this is not entirely clear. This decomposition of **2** occurs only upon the application of a potential to the solution, generating $[\mathrm{Mn^{III}Mn^{IV}}(\mu\text{-O})_2(\mathrm{bpy})_4]^{3+}$ (**1**) and a manganese(II) species in the electroactive layer. A plausible pathway for this reaction is shown in eqs 4 and 5. Further support for the formation of **1** is given by a study of the zero current potential (ZCP) curve for the complex. The ZCP curve of **2** in pH 4.55 phosphate buffer, shown in Figure

---

[13] Brudvig, G. W. In *Advanced EPR, Applications in Biology and Biochemistry*; Hoff, A. J., Ed.; Elsevier: Amsterdam, 1989.

[14] Ghosh, P. K.; Brunschwig, B. S.; Chou, M.; Creutz, C.; Sutin, N. *J. Am. Chem. Soc.* **1984**, *106*, 4772.

[15] Cabaniss, G. E.; Diamantis, A. A.; Murphy, W. R., Jr.; Linton, R. W.; Meyer, T. J. *J. Am. Chem. Soc.* **1985**, *107*, 1845.

$$\mathrm{Mn^{IV}{}_2(\mu\text{-}O)_2(\mu_2\text{-}HPO_4)(bpy)_2(H_2PO_4)_2 + e^- \rightarrow Mn^{IV}Mn^{III}(\mu\text{-}O)_2(\mu_2\text{-}HPO_4)(bpy)_2(H_2PO_4)_2} \quad (4)$$

$$\mathrm{Mn^{IV}Mn^{III}(\mu\text{-}O)_2(\mu_2\text{-}HPO_4)(bpy)_2(H_2PO_4)_2 + 2bpy \rightarrow Mn^{III}Mn^{IV}(\mu\text{-}O)_2(bpy)_4{}^{3+} + 3H_3PO_4} \quad (5)$$

5, suggests that the species generated at the electrode surface is $[\mathrm{Mn^{III}Mn^{IV}(\mu\text{-}O)_2(bpy)_4}]^{3+}$. The ZCP of **2** is the same as $E_{1/2}$ of the bpy dimer **1** (0.71 ± 0.05 V) at that pH. Addition of pure $[\mathrm{Mn^{III}Mn^{IV}(\mu\text{-}O)_2(bpy)_4}]^{3+}$ dimer to the solution of **2** in pH 4.5 phosphate buffer generated no new feature in the cyclic voltammogram. On the basis of this evidence, we assign the peak at around 0.7 V to the (III,IV)/(III,III) couple of **1**.[7] The peak at ~0.0 V is assigned to a Mn(II)/Mn(III) couple on the basis of CV measurements of Mn(II) in 0.1 M H_3PO_4 at pH = 4.5.

The electrochemistry of the Mn(III) complex **3** was found to be surprisingly similar to that observed for **2**. There was a quasi-reversible couple at ~0.7 V and a broad peak ~0.0 V. The Pourbaix diagram of **3** in phosphate buffer again shows that there is a linear relationship of $E_{1/2}$ with pH. The slope of 0.077 ± 0.01 V/pH (R = 0.989) clearly shows that a proton-coupled electron-transfer mechanism is operative. The EPR spectrum of a solution of **3** in 0.1 M H_3PO_4 shows the six-line spectrum indicative of the presence of copious Mn(II) even before any voltage was applied to the solution; the visible spectrum of this solution shows a distinct 610-nm peak attributable to the (IV,IV) dimer, **2**. This indicates that **3** is undergoing a disproportionation in solution which generates the (IV,IV) complex, **2**. Quantitative analysis of the intensity of the 610-nm absorbance indicates that disproportionation, $\mathbf{3} \rightarrow \mathbf{2} + 2\mathrm{Mn}^{2+}$, was virtually complete in this solution (~0.1 mM **3**). EPR studies show that there is no appreciable increase in the concentration of Mn(II) with time for this solution, once **3** has dissolved; this means that the disproportionation process is essentially instantaneous and complete as soon as the complex dissolves in the phosphate medium and the observed electrochemistry is that of the (IV,IV) dimer **2**.

A solution of the pure Mn(III) complex **3** in 0.1 M H_3PO_4 disproportionates immediately, yielding **2** and Mn(II). However, the electrochemistry of **2** at a glassy-carbon electrode in 0.1 M H_3PO_4 is indicative of the formation of the (III,IV) dimer **1** in the electroactive layer on the application of potential. The conversion of **2** to **1** in the electroactive layer by reduction (eqs 4 and 5) requires the presence of available free bpy ligand which concentrates on the glassy-carbon electrode surface by adsorption, a process known to occur on this type of electrode.[16] Even though bpy adsorption on the glassy-carbon electrode is a problem, other electrodes, such as SnO_2 or In_2O_3, have been shown to provide poorer peak resolution for the CV of such manganese clusters;[16] the glassy-carbon electrode pretreatment which permits sharpening of CV waves makes it the best choice for our studies.

This effective increase in the concentration of bpy in the region of the electroactive layer mimics the conditions which occur when pH 4.5 bpy buffer is added to a solution of **1** in 0.1 M H_3PO_4 (note that this solution contains a mixture of a (IV,IV) dimer **2** and a Mn(III) species); upon addition of pH 4.5 bpy buffer to the 0.1 M H_3PO_4 solution, the mixed-valence di-μ-oxo dimer, **1**, is quantitatively regenerated as determined from EPR and UV–vis spectroscopy. The electrochemical reduction of **2** causes bpy to be taken up from the electrode surface to generate **1**; hence, solutions of **2** exhibit the electrochemistry of **1** plus Mn(II). This chemistry demonstrates the thermodynamic stability of the (III,IV) dimer **1**.

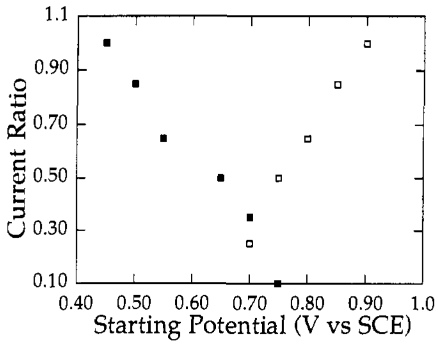

Figure 5. Zero current potential curve for $[\mathrm{Mn^{IV}Mn^{IV}(\mu\text{-}O)_2(\mu\text{-}HPO_4)(bpy)_2(H_2PO_4)_2}]$ in 0.1 M phosphate buffer at pH 4.55. ZCP: 0.71 ± 0.01 V. Scan rate: 100 mV/s.

Summary. Phosphate clearly stabilizes Mn(IV) in aqueous solution. With aqueous acetate ion, a (III,IV) dimer with a $[\mathrm{Mn^{III}Mn^{IV}(\mu\text{-}O)_2(CH_3CO_2)}]^{2+}$ core is the most oxidized dimeric species that has been isolated;[17] no (IV,IV) dimer containing bridging acetate has been isolated. From nonaqueous solutions, (III,III) dimers possessing the $[\mathrm{Mn^{III}Mn^{III}(\mu\text{-}O)(CH_3CO_2)_2}]^{2+}$ core have been characterized.[18] The facile acid-catalyzed disproportionation of a (III,IV) bipy dimer (**1**) to produce a (IV,IV) dimer and some lower valence manganese species in acidic phosphate medium may have some relevance to the assembly of the Mn cluster in PS II. It is known that protons are liberated during certain of the photooxidation events in the water oxidation cycle. These protons which are produced in the immediate vicinity of the water oxidation Mn catalyst help to determine the local pH there. Such pH alterations may help to stabilize oxidation equivalent buildup in PS II by promoting disproportionation to even higher valence for some Mn atoms and reduction of others to more photochemically active, easier to oxidize lower valent forms for other manganese centers. Such facile acid-catalyzed disproportionation seems to be fairly common in high-valent manganese chemistry.[17,19]

Another feature of high-valent manganese chemistry that we see is the lability of the metal ion's coordination sphere in aqueous solution. While Mn(II) is labile to substitution, the higher oxidation states are usually considered to be more inert.[3] Our observations demonstrate that the higher oxidation states of manganese can also be quite labile in aqueous solution. The facile quantitative reconversion of a solution of **2** and **3** back to **1** with the addition of pH 4.5 bpy buffer and the rapid disproportionation of the Mn(III) complex **3** on dissolving in aqueous H_3PO_4 to give the (IV,IV) dimer **2** and Mn(II) exemplify this point. It would seem that electron exchange with lower-valent Mn present in solution helps to make the high-valent species more labile.

Acknowledgment. This research was supported by funds from the Research Corp. (J.E.S.) and the Cooperative State Research Service, U.S. Department of Agriculture (G.W.B. and R.H.C.); L.J.B. thanks Pfizer Corp. for summer fellowship support. We thank Professor M. Ditzler of College of the Holy Cross for the diffuse reflectance spectral measurements. Helpful discussions with Professors J. W. Faller and H. H. Thorp are gratefully acknowledged.

Supplementary Material Available: Text describing crystallographic procedures and tables of crystallographic data, atomic coordinates and isotropic thermal parameters, bond distances and angles, and non-hydrogen anisotropic thermal parameters (14 pages). Ordering information is given on any current masthead page.

---

(16) Thorp, H. H.; Bowden, E. F.; Brudvig, G. W. *J. Electroanal. Chem.* **1990**, *290*, 293.

(17) Wieghardt, K.; Bossek, U.; Nuber, B.; Weiss, J.; Bonvoisin, J.; Corbella, M.; Vitols, S. E.; Girerd, J.-J. *J. Am. Chem. Soc.* **1988**, *110*, 7398.

(18) (a) Ménage, S.; Girerd, J.-J.; Gleizes, A. *J. Chem. Soc., Chem. Commun.* **1988**, 431. (b) Bashkin, J. S.; Schake, A. R.; Vincent, J. B.; Chang, H.-R.; Li, Q.; Huffman, J. C.; Christou, G.; Hendrickson, D. *J. Chem. Soc., Chem. Commun.* **1988**, 700. (c) Sheats, J. E.; Czernuszewicz, R. S.; Dismukes, C. S.; Rheingold, A. L.; Petrouleas, V.; Stubbe, J.; Armstrong, W. H.; Beer, R. H.; Lippard, S. J. *J. Am. Chem. Soc.* **1987**, *109*, 1435.

(19) Sarneski, J. E.; Thorp, H. H.; Brudvig, G. W.; Crabtree, R. H.; Schulte, G. K. *J. Am. Chem. Soc.* **1990**, *112*, 7255.